

# Vibrational Collective Dynamics of Dry Proteins in the Terahertz Region

Alessandro Paciaroni,<sup>\*,†,‡</sup> Andrea Orecchini,<sup>†,‡,||</sup> Michael Haertlein,<sup>||</sup> Martine Moulin,<sup>||</sup> Valeria Conti Nibali,<sup>⊥</sup> Alessio De Francesco,<sup>§</sup> Caterina Petrillo,<sup>†,‡</sup> and Francesco Sacchetti<sup>†,‡</sup>

<sup>†</sup>Dipartimento di Fisica, Università degli Studi di Perugia, Via Pascoli, I-06123 Perugia, Italy

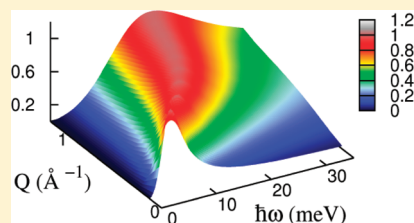
<sup>‡</sup>Istituto Officina dei Materiali, Unità di Perugia, c/o Dipartimento di Fisica, Università di Perugia, I-06123 Perugia, Italy

<sup>§</sup>CNR, Istituto Officina dei Materiali, Unità di Grenoble, Institut Laue Langevin, 6 rue J. Horowitz, F-38042 Grenoble, France

<sup>||</sup>Institut Laue Langevin, 6 rue J. Horowitz, F-38042 Grenoble, France

<sup>⊥</sup>Dipartimento di Fisica, Università degli Studi di Messina, via Salita Sperone, I-98166 Messina, Italy

**ABSTRACT:** The coherent density fluctuations of a perdeuterated dry protein have been studied by Brillouin neutron spectroscopy. Besides a nearly wavevector-independent branch located around 5 meV, a propagating mode with a linear trend at low wavevector  $Q$  is revealed. The corresponding speed of  $3780 \pm 130$  m/s is definitely higher than that of hydrated proteins. Above  $Q = 0.8 \text{ \AA}^{-1}$ , this mode becomes overdamped, with lifetimes shorter than 0.1 ps, in fashion similar to glassy materials. The present results indicate that dry proteins sustain coherent density fluctuations in the THz frequency regime. The trend of the longitudinal modulus indicates that in this frequency range dry biomolecules are more rigid than hydrated proteins.



## INTRODUCTION

Conformational changes occurring on the micro- and millisecond time scale of proteins are the subject of a huge body of literature, as they govern progress along various biological activities such as enzyme catalysis and ligand binding events.<sup>1–3</sup> Less is known about faster thermal fluctuations, which involve single-particle and collective motions in the picosecond time scale and are supposed to initiate and modulate the slower dynamical processes mentioned above.<sup>4</sup> In fact, the biological activity of proteins requires a delicate and precise balance between flexibility and stability. For many processes with characteristic times longer than a few picoseconds, bulk-like components of motion appear in the dynamics of the protein, due to the restoring forces that stabilize their native structures. The frequencies and amplitudes of protein intramolecular motions are directly related to the mechanical part of their free energy and, ultimately, to their elastic properties.<sup>5–8</sup> However, over short time scales (less than 0.5 ps), the small-amplitude protein internal motions are reminiscent of the high-frequency motions of molecules in a disordered environment, such as molecular liquids.<sup>9</sup> Each atomic group temporarily rattles in a cage that consists of either neighboring protein groups or molecules of the surrounding solvent, the cage itself being of course not stationary.<sup>4</sup> The frequent and random collisions between protein groups are the microscopic basis of the frictional effects that limit the rate of the net displacement of the group.<sup>10</sup>

Inelastic neutron<sup>11</sup> and X-ray<sup>12–14</sup> scattering experiments have shown that hydrated proteins support collective density fluctuations similar to those existing in liquids and disordered

matter. Yet, the intimate nature of this short-wavelength collective dynamics is still far from being clear: neither are known if coherent excitations can propagate through the dry protein system nor if the role of the solvent has been completely elucidated,<sup>15,16</sup> although the propagation of collective excitations in protein hydration water was recently observed.<sup>16</sup>

In this context, we report the results of a Brillouin neutron scattering investigation on perdeuterated maltose binding protein (MBP) in the dry powder state. We show that the system is able to sustain propagating modes in the THz range, with a damping character similar to glass-like systems.

## MATERIALS AND METHODS

**Sample Preparation.** The propagation of coherent density fluctuations through the protein macromolecule can be properly studied only provided that a fully deuterated protein sample is available. Indeed, in isotopically natural proteins, the contribution to the neutron scattering signal comes mainly from the incoherent scattering of hydrogen atoms. These atoms are abundantly and uniformly present in every protein and have a very large incoherent neutron cross-section (about 80 barns for thermal neutrons) that overcomes by far both its coherent component ( $\sim 2$  barns) and the mainly coherent cross-sections of all other protein atoms ( $\sim 5$  barns for C, O, N, and S). In addition, in the small- $Q$  region, the negative scattering length of

**Received:** November 21, 2011

**Revised:** February 28, 2012

**Published:** February 28, 2012

hydrogen (−3.74 fm) tends to cancel the coherent scattering of all the other atoms, so that an isotopically natural protein is of little use to study coherent dynamics.<sup>17,18</sup> On the contrary, deuterium atoms predominantly diffuse neutrons with a positive coherent scattering length of 6.7 fm, thus providing access to collective dynamics.<sup>18</sup> Perdeuterated MBP was produced by the ILL-Deuteration Laboratory (Grenoble, France) for the first time in the large amount of about 1 g, which is necessary to perform the challenging measurement of the small inelastic coherent response. The sample was measured at room temperature. The correct preservation of the native status of the protein was checked both before and after exposure to the neutron beam.

**Inelastic Neutron Scattering.** The neutron scattering experiment was carried out at the Brillouin spectrometer BRISP (ILL, Grenoble, France). The experimental setup provided access to a  $Q$  range from 0.2 to 1.4 Å<sup>−1</sup> and wide enough energy range (some tens of meV) thanks to the rather high incoming neutron energy of 83.7 meV, with an energy resolution of 2.6 meV. Before any data analysis, the raw spectra were subtracted of empty cell and environmental background contributions, corrected for self-absorption and normalized to a vanadium standard. The dynamical structure factor  $S(Q, E)$ , as a function of the momentum and energy transfer,  $\hbar Q$  and  $E$  respectively, was derived through straight kinematical relationships from the acquired raw spectra. As the sample here is an isotropic powder,  $S(Q, E)$  depends only on the wavevector modulus  $Q$ . A high value of about 0.9 was achieved for the transmission coefficient of the sample. Multiple scattering was calculated according to the approach successfully used in previous experiments<sup>19</sup> and subtracted from the present data, although such correction is fairly small in this low-scattering sample.

In the investigated  $Q$ -range, coherent scattering comes from protein density fluctuations occurring over distances  $d$  of the order of tens of Å, and the dynamical structure factor is the frequency spectrum of the correlations between the density fluctuations of a given wavevector  $Q \approx 2\pi/d$ .<sup>18</sup> In an ideal crystal, such density fluctuations can be rigorously classified in terms of  $Q$ -dependent eigenmodes (phonons). In the present disordered system, the eigenmodes cannot be numbered using the wave vector  $Q$ ; therefore, the spectra at constant  $Q$  will be characterized by rather broadened inelastic features. The observed width can be connected to both the structural disorder and the finite lifetime of the eigenmodes due to the interaction with other excitations.

The experimental  $S(Q, E)$  can be modeled in a simplified way by a phenomenological function already used in previous investigations as follows:<sup>16,19,20</sup>

$$S(Q, E) = \left\{ a(Q)\delta(E) + (n(E) + 1) \frac{E}{\pi k_B T} \times \sum_{i=1}^2 a_i(Q) \frac{\hbar \Gamma_i(Q) \hbar^2 \Omega_i^2(Q)}{[(E^2 - \hbar^2 \Omega_i^2(Q))^2 + (\hbar \Gamma_i(Q) E)^2]} \right\} * R(Q, E) \quad (1)$$

where the first  $a(Q)\delta(E)$  term accounts for the elastic and quasielastic contributions, known to be much sharper than the instrument resolution, to which two distinct damped harmonic oscillator (DHO) response functions are added, each one characterized by  $Q$ -dependent weight  $a_i(Q)$ , excitation energy  $\hbar \Omega_i(Q)$  and damping factor  $\hbar \Gamma_i(Q)$ , and  $n(E)$  being the Bose thermal factor. DHO functions have been often used to describe the coherent inelastic modes of biological systems in

light scattering,<sup>21,22</sup> X-ray,<sup>12</sup> and neutron spectroscopy.<sup>16</sup> These functions provide a simplified representation of collective density fluctuations occurring in fluids and disordered matter.<sup>8,23,24</sup> In fact, due to the protein structural and dynamical heterogeneity, i.e., the huge variety of intramolecular geometrical environments and degrees of freedom, each DHO function can be regarded as a broad, almost continuous distribution of density fluctuations. For this reason, the  $\hbar \Omega_i(Q)$  and  $\hbar \Gamma_i(Q)$  parameters represent, respectively, the average excitation energy and damping factor of a whole class of collective motions possibly sustained by the system. Both the elastic and the inelastic terms in eq 1 are convoluted with the experimental energy resolution function  $R(Q, E)$ .

## RESULTS AND DISCUSSION

Before discussing the details of the inelastic spectral features of dry MBP, a first evaluation of the quality and consistency of our data can be obtained by an inspection of the sample static structure factor, which was derived by the equation  $S(Q) = \int S(Q, E) dE$  and is displayed in Figure 1. A rather intense

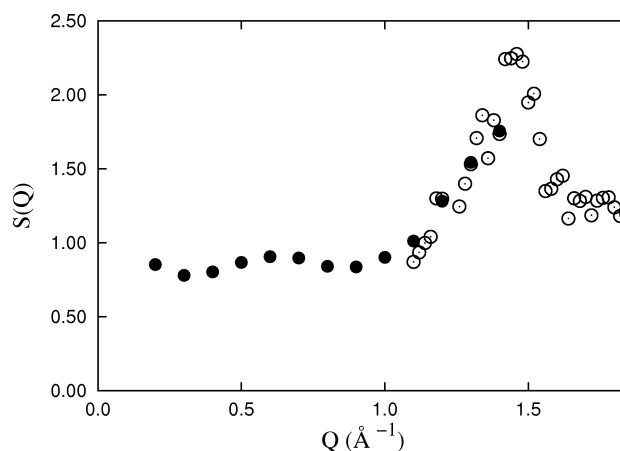


**Figure 1.** Static structure factor  $S(Q)$  of dry MBP. The data from the present experiment on BRISP (full circles) are complemented with data from IN4 (time-of-flight spectrometer at ILL, Grenoble) to expand the  $Q$  range (empty circles).

diffraction peak is well visible at 1.4 Å<sup>−1</sup>. It can be ascribed to the constructive interference between nonbonded residues,<sup>25</sup> i.e., residues that are not near neighbors in the primary structure, but close to each other in the three-dimensional configuration, whose average distance in proteins is typically ~4.5 Å. In addition, a weak bump can be identified at 0.6 Å<sup>−1</sup>, likely due to the center-to-center  $\alpha$  helix packing distance.<sup>26</sup> These features were already observed in few other proteins investigated by neutron<sup>27</sup> and X-ray<sup>12–14</sup> scattering and by numerical simulations,<sup>25</sup> which corroborates the quality of our data and the overall reliability of the applied correction procedure.

As concerns the inelastic behavior of dry MBP, the dynamical structure factor is shown in Figure 2a,b for the two different  $Q$ -values 0.5 and 1.1 Å<sup>−1</sup>. The inelastic signal of the protein density fluctuations appears as a small but clear double shoulder rising well outside the tails of the Gaussian-shaped elastic peak, which is defined by the experimental energy resolution. The quality of the data is quite satisfactory and is actually the best that can currently be achieved via state-of-the-art Brillouin neutron scattering. Indeed, the absence of sharper inelastic

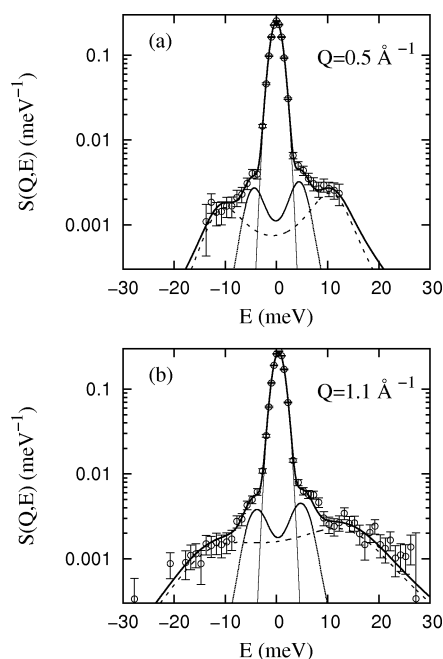


**Figure 2.** (a) Dynamical structure factor of dry MBP at  $Q = 0.5 \text{ \AA}^{-1}$  with the two fitting components, the narrow central energy resolution curve (thin line) and the total fitting curve (thick line). (b) Same as that in panel a but at the different  $Q$ -value of  $Q = 1.1 \text{ \AA}^{-1}$ .

peaks is due to intrinsic properties of the system, as is well-known from few other Brillouin investigations on similar disordered samples.<sup>11–14,16,24,28</sup> In fact, this is further confirmed by several other experimental techniques, such as incoherent neutron scattering,<sup>29–31</sup> far-infrared,<sup>32,33</sup> Raman,<sup>34</sup> and terahertz<sup>35–37</sup> spectroscopies, which have shown that no sharp inelastic feature can be found in the protein vibrational density of states below 40 meV. This happens because, at variance with small molecular systems where the vibrational resonances are widely spaced and relatively narrow, the collective vibrational modes of complex macromolecules become dense, and individual modes overlap with each other. In addition, in this lower-frequency range, the modes get delocalized and involve the motion of larger groups of atoms. The coherent inelastic contribution observed herewith was not revealed by previous X-ray scattering measurements of dry lysozyme,<sup>13</sup> probably due to the long Lorentzian tails of the energy resolution function. On the contrary, an inelastic coherent signal had already been observed in dry perdeuterated C-phycoerythrin by neutron triple-axis spectroscopy, although the double spectral feature was not resolved, likely due to the limited statistics at that time.<sup>11</sup>

Already from a first inspection of Figure 2, the low-energy shoulder appears constantly located around 5 meV, while the position of the second peak seems to shift toward higher energies and broaden on passing from 0.5 to 1.1  $\text{\AA}^{-1}$ . The spectra are described quite well by eq 1, with the two DHO components properly fitting the inelastic features. The nature of the two inelastic components is further clarified by the  $Q$ -dependence of their characteristic excitation energies, i.e., the dispersion curves  $\hbar\Omega_i(Q)$ , which are shown in Figure 3a. The low-energy mode is confirmed to behave as a nearly  $Q$ -independent branch located at slightly less than 5 meV. Quite interestingly, the high-energy mode displays a dispersive character, spanning the energy range between 5 and 20 meV

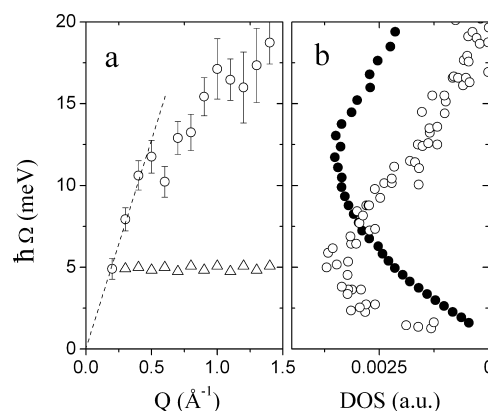


**Figure 3.** (a) Low-energy DHO excitation energy (empty triangles) and high-energy DHO excitation energy (empty circles). The line is a linear fit in the  $Q$  range from 0.2  $\text{\AA}^{-1}$  to 0.5  $\text{\AA}^{-1}$ . (b) Generalized vibrational density of states (full circles) measured on the time-of-flight spectrometer IN4 (ILL, Grenoble) on dry MBP, with an incident wavelength of 2.2  $\text{\AA}$ . This density of states has been estimated in the high- $Q$  region to reduce coherent distortions with the formula  $6E/[Q^2(1 - \exp(-E/k_B T))] S(Q,E)$ . Vibrational density of normal modes of globular proteins (empty circles) from ref 40. For the sake of clarity, the two densities of states are plotted on different arbitrary scales.

with an initial linear trend in the low- $Q$  region. It is worth to remark that, considering the involved  $Q$ -range, the two excitations have short subnanometric and nanometric wavelengths  $\lambda = 2\pi/Q$  lying in the range 4.5/30  $\text{\AA}$ . We also notice that the dispersion curve of the high-energy mode shows a shallow minimum at about 0.6  $\text{\AA}^{-1}$  and a flattening toward 1.5  $\text{\AA}^{-1}$ , just in correspondence to, respectively, the small bump and the main diffraction peak observed in the protein structure factor shown in Figure 1. This behavior suggests that the protein medium and short-range order affects the dispersion curve in analogy to the Brillouin zone in crystals.

Figure 3b shows that in the low-energy region below 20 meV the generalized vibrational density of states of dry MBP is characterized by a broad bump centered at around 12 meV, a feature already observed in several proteins.<sup>29,38–40</sup> Both modes observed in the experimental dispersion curves directly contribute to this bump, although it is difficult to single out their individual signatures in the density of states because of their large  $Q$ -dependent damping factor (see below). In Figure 3b, we also report the calculated low-energy density of normal modes for several globular proteins, which fall into a universal curve centered at approximately 5 meV.<sup>41</sup> Apart from the usual harmonic hypothesis of normal mode methods, such density of states was calculated under the strict approximation that bond lengths are frozen and only changes in rotational angles are allowed.<sup>42</sup> Therefore, we may suppose the low-frequency mode observed in our experimental dispersion curves to be directly related to torsion-angle protein normal modes.

The low- $Q$  slope of the dispersive branch provides the longitudinal speed of the relative propagating excitations, which, calculated on the  $Q$  range up to 0.5  $\text{\AA}^{-1}$ , turns out to be  $c_L = 3780 \pm 130 \text{ m/s}$ . Such a velocity is definitely higher than the value of about  $2000 \pm 30 \text{ m/s}$  that we measured by an in-house ultrasound apparatus, in agreement with what observed in a compacted disk of dry lysozyme.<sup>43</sup> This phenomenon of collective excitations propagating much faster in the THz than in the MHz frequency range is reminiscent of the so-called fast sound observed in bulk water,<sup>19,20,44</sup> where it

is considered to originate from the fact that at high frequencies the dynamical response of the liquid becomes solid-like. The transition between ordinary and fast sound in water is supposed to take place in the  $Q$ -range between 0.01 and 0.3  $\text{\AA}^{-1}$ .<sup>45</sup> We may speculate that the similar and unexpected transition in dry MBP powders may have the same microscopic origin as in bulk water.

As water is the physiological environment to proteins, it is natural to compare the features of the collective motions of these two kinds of systems, in order to find possible channels for the low-frequency vibrational coupling between them. The protein mode at 5 meV has an analogous counterpart in bulk water at the slightly higher energy of 6 meV, this peak being reminiscent of the collective transverse acoustic mode TA1 of the hydrogen-bond network in ice, i.e., the O–O–O bending motion.<sup>46</sup> However, the propagation speed of the high-frequency mode in the dry protein is much larger than in bulk water, i.e.,  $3040 \pm 80$  m/s,<sup>20</sup> and even larger than in low- and high-density amorphous ice, where the speed is  $3550 \pm 50$  m/s.<sup>47</sup>

Further quantitative information about the nature of collective modes in dry MBP can be obtained by the ratio between their damping factors and excitation energies. For the low-energy mode, such ratio has a nearly constant value of about 0.5, while for the propagating mode, it turns out to be linear in the whole investigated  $Q$ -range, as it can be seen in Figure 4. The latter mode is definitely overdamped above 0.8

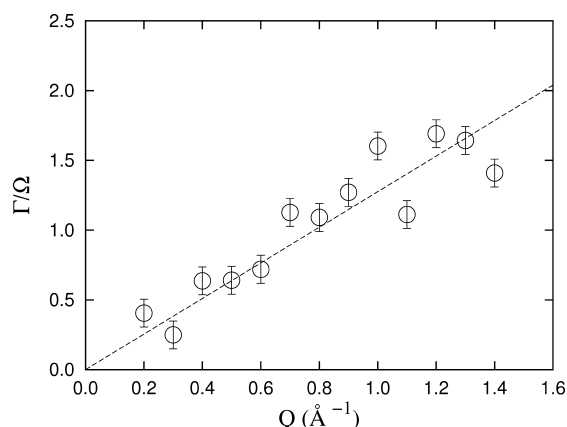


**Figure 4.** Ratio between the damping factor  $\hbar\Gamma$  and the excitation energy  $\hbar\Omega$  of the propagating mode. The straight line is a guide for the eye.

$\text{\AA}^{-1}$ , with a lifetime of only  $2/\hbar\Gamma = 0.1$  ps, which corresponds to a mean free path  $2c_L/\hbar\Gamma$  of a few angstroms. On the contrary, excitations with decreasing wavevector from 0.5 to 0.2  $\text{\AA}^{-1}$  propagate over a spatial range from 10  $\text{\AA}$  to 30  $\text{\AA}$  before vanishing. In the moderately low- $Q$  region, where  $\hbar\Omega(Q)$  follows a linear trend vs  $Q$ , the damping factor of the high-energy mode shows a quadratic dependence, a behavior similar to that found in biological water<sup>16,48</sup> and in several glassy systems.<sup>24,28</sup> Such a common behavior further supports the so-called protein–glass analogy.<sup>49</sup>

The large number of internal degrees of freedom within a protein molecule allows to describe its general dynamic properties in terms of bulk quantities, such as packing density, compressibility, or other elastic coefficients, which are typically considered for macroscopic systems.<sup>50</sup> The estimated high-frequency longitudinal velocity  $c_L$  can thus be employed to

directly calculate the longitudinal moduli  $M$ , which is in turn related to the adiabatic bulk and shear moduli  $K$  and  $G$  via the following relationship:

$$M = \rho c_L^2 = K + 4/3G \quad (2)$$

where  $\rho$  is the mass density.  $M$  is equivalent to the adiabatic elastic stiffness constant of crystals and therefore provides an estimate of the average rigidity of the material, i.e., its resistance to volumetric and shear stress. With a protein mass density of 1.4 g/cm<sup>3</sup>,<sup>3,51</sup> the longitudinal modulus of the protein alone turns out to be 20 GPa, definitely higher than bulk water (9 GPa). We can compare the elastic properties of the dry protein with those of cytochrome *c* hydrated at 0.2*h* (*h* = grams of water/grams of protein)<sup>14</sup> and of  $\beta$ -lactoglobulin at 0.5*h* and 1.0*h*,<sup>13</sup> where the longitudinal velocities, as measured by inelastic X-ray scattering, result to be  $3458 \pm 42$  m/s,  $2900 \pm 160$  m/s, and  $2860 \pm 110$  m/s, respectively. If we suppose these proteins to have elastic average behavior and mass density similar to MBP,<sup>51</sup> we find that the 20 GPa longitudinal modulus of the dry system decreases to 16, 11, and 11 GPa when the hydration level increases from 0*h* to 0.2*h*, 0.5*h*, and 1.0*h*, respectively. The decreasing trend of  $M$  with increasing hydration level suggests that the addition of water makes the system less stiff, i.e., improves the protein ability to respond to mechanical stress. A dry protein would behave as a rather stiff system, while the hydrated protein would be much prompter to possible mechanical stimuli by solvent or ligands, with the relevant consequences for the onset of biological functionality. In fact, the deformability of the protein interior can provide a reservoir of energy in the intermediate steps of a catalytic pathway and is also crucial for the creation of internal cavities, which are in turn involved in a number of intramolecular dynamic processes.<sup>7</sup> Therefore, the hydration-dependence of the protein rigidity suggests that all these phenomena require a certain water content to be activated or to speed up their rate. The present results are consistent with a picture where the solvent enhances the biomolecule semiliquid-like character on increasing the mobility of protein side chains at the interface with water.<sup>52,53</sup>

## CONCLUSIONS

By inelastic neutron scattering measurements, we could reveal the internal collective vibrational dynamics of dry perdeuterated MBP in the terahertz frequency region. The dispersion curves consist of a low-energy localized mode at about 5 meV and of a high-energy mode propagating over a few tens of angstroms with the remarkable speed of about 3800 m/s. On one hand, such double-excitation pattern is a property that proteins share with bulk and biological water.<sup>16,20</sup> Thus, it might be speculated that such vibrational modes represent a channel for solvent–biomolecule dynamical coupling, known to ultimately play a role in biological activity. In addition, the rather high speed of the propagating mode in the *dry* state of the protein, with respect to that measured in some *hydrated* proteins, suggests a progressive reduction of protein stiffness upon hydration, with a consequent increase of flexibility, which is known to be connected to the activation of biological function upon hydration.

## AUTHOR INFORMATION

### Corresponding Author

\*E-mail: alessandro.paciaroni@fisica.unipg.it.



## Notes

The authors declare no competing financial interest.

## REFERENCES

- (1) Henzler-Wildman, K.; Kern, D. *Nature* **2007**, *450*, 964–972.
- (2) Boekelheide, N.; Salomon-Ferrer, R.; Miller, T. F. III. *Proc. Natl. Acad. Sci. U.S.A.* **2011**, *108*, 16159–16163.
- (3) Osborne, M. J.; Schnell, J.; Benkovic, S. J.; Dyson, H. J.; Wright, P. E. *Biochemistry* **2001**, *40*, 9846–9859.
- (4) McCammon, J. A. *Rep. Prog. Phys.* **1984**, *47*, 1–46.
- (5) Cooper, A. *Proc. Natl. Acad. Sci. U.S.A.* **1976**, *73*, 2740–2741.
- (6) Morozov, V. N.; Morozova, T. Y. *J. Biomol. Struct. Dyn.* **1993**, *11*, 459–481.
- (7) Kharakoz, D. P. *Biophys. J.* **2000**, *79*, 511–525.
- (8) Kobayashi, N.; Yamato, T.; Go, N. *Proteins: Struct., Funct., Genet.* **1997**, *28*, 109–116.
- (9) Hansen, J.-P.; McDonald, R. *Theory of Simple Liquids*; Academic Press: London, U.K., 2006.
- (10) McCammon, J. A.; Gelin, B. R.; Karplus, M. *Nature* **1977**, *267*, 585–590.
- (11) Bellissent-Funel, M.-C.; Teixeira, J.; Chen, S.-H.; Dorner, B.; Middendorf, H. D.; Crespi, H. L. *Biophys. J.* **1989**, *56*, 713–716.
- (12) Liu, D.; Chu, X.-Q.; Lagi, M.; Zhang, Y.; Fratini, E.; Baglioni, P.; Atlas, A.; Said, A.; Alp, E.; Chen, S.-H. *Phys. Rev. Lett.* **2008**, *101*, 135501.
- (13) Yoshida, K.; Hosokawa, S.; Baron, A. Q. R.; Yamaguchi, T. J. *Chem. Phys.* **2010**, *133*, 13450.
- (14) Leu, B. M.; Alatas, A.; Sinn, H.; Alp, E. E.; Said, A. H.; Yavaş, H.; Zhao, J.; Sage, J. T.; Sturhahn, W. *J. Chem. Phys.* **2010**, *132*, 085103.
- (15) Paciaroni, A.; Orecchini, A.; Cornicchi, E.; Marconi, M.; Petrillo, C.; Haertlein, M.; Moulin, M.; Schober, H.; Tarek, M.; Sacchetti, F. *Phys. Rev. Lett.* **2008**, *101*, 148104.
- (16) Orecchini, A.; Paciaroni, A.; De Francesco, A.; Petrillo, C.; Sacchetti, F. *J. Am. Chem. Soc.* **2009**, *131*, 4664–4669.
- (17) Zaccai, G.; Jacrot, B. *Annu. Rev. Biophys. Bioeng.* **1983**, *12*, 139–157.
- (18) Lovesey, S. *Theory of Neutron Scattering from Condensed Matter*; Oxford University Press: Oxford, U.K., 1988.
- (19) Petrillo, C.; Sacchetti, F.; Dorner, B.; Suck, J.-B. *Phys. Rev. E* **2000**, *62*, 3611–3618.
- (20) Sacchetti, F.; Suck, J.-B.; Petrillo, C.; Dorner, B. *Phys. Rev. E* **2004**, *69*, 061203.
- (21) Colaianni, S. E. M.; Nielsen, O. F. *J. Mol. Struct.* **1995**, *347*, 267–284.
- (22) Urabe, H.; Sugawara, Y.; Ataka, M.; Rupprecht, A. *Biophys. J.* **1998**, *74*, 1533–1540.
- (23) Bafle, U.; Guarini, E.; Barocchi, F. *Phys. Rev. E* **2006**, *73*, 061203.
- (24) Monaco, G.; Giordano, V. M. *Proc. Natl. Acad. Sci. U.S.A.* **2009**, *106*, 3659–3663.
- (25) Bahar, I.; Jernigan, R. L. *J. Mol. Biol.* **1997**, *266*, 195–214.
- (26) Hirai, M.; Koizumi, M.; Hayakawa, T.; Takahashi, H.; Abe, S.; Hirai, H.; Miura, K.; Inoue, K. *Biochemistry* **2004**, *43*, 9036–9049.
- (27) Gaspar, A. M.; Busch, S.; Appavou, M.-S.; Haeussler, W.; Georgii, R.; Su, Y.; Doster, W. *Biochim. Biophys. Acta* **2010**, *1804*, 76–82.
- (28) Rufflé, B.; Guimbretière, G.; Courtens, E.; Vacher, R.; Monaco, G. *Phys. Rev. Lett.* **2006**, *96*, 045502.
- (29) Cusack, S.; Doster, W. *Biophys. J.* **1990**, *58*, 243–251.
- (30) Middendorf, H. D.; Hayward, R. L.; Parker, S. F.; Bradshaw, J.; Miller, A. *Biophys. J.* **1995**, *69*, 660–673.
- (31) Paciaroni, A.; Stroppolo, M. E.; Arcangeli, C.; Bizzarri, A. R.; Desideri, A.; Cannistraro, S. *Eur. Biophys. J.* **1999**, *28*, 447–456.
- (32) Paciaroni, A.; Bizzarri, A. R.; Cannistraro, S. *J. Mol. Liq.* **2000**, *84*, 3–16.
- (33) Leyser, H.; Doster, W.; Diehl, M. *Phys. Rev. Lett.* **1999**, *14*, 2987–2991.
- (34) Xie, A.; van der Meer, A. F.; Austin, R. H. *Phys. Rev. Lett.* **2002**, *88*, 018102.
- (35) Caliskan, G.; Kisliuk, A.; Tsai, A. M.; Soles, C. L.; Sokolov, A. P. *J. Chem. Phys.* **2003**, *118*, 4230–4236.
- (36) Ebbinghaus, S.; Kim, S. J.; Heyden, M.; Yu, X.; Heugen, U.; Gruebele, M.; Leitner, D. M.; Havenith, M. *Proc. Natl. Acad. Sci. U.S.A.* **2007**, *104*, 20749–20752.
- (37) Kistner, C.; André, A.; Fischer, T.; Thoma, A.; Janke, C.; Bartels, A.; Gisler, T.; Maret, G.; Dekorsy, T. *Appl. Phys. Lett.* **2007**, *90*, 233902.
- (38) Yunfen, H.; Chen, J.-Y.; Knab, J. R.; Zheng, W.; Markelz, A. G. *Biophys. J.* **2011**, *100*, 1058–1065.
- (39) Orecchini, A.; Paciaroni, A.; Bizzarri, A. R.; Cannistraro, S. *J. Phys. Chem. B* **2001**, *105*, 12150–12156.
- (40) Wood, K.; Caronna, C.; Fouquet, P.; Haussler, W.; Natali, F.; Ollivier, J.; Orecchini, A.; Plazanet, M.; Zaccai, G. *Chem. Phys.* **2008**, *345*, 305–314.
- (41) Balog, E.; Perahia, D.; Smith, J. C.; Merzel, F. *J. Phys. Chem. B* **2011**, *115*, 6811–6817.
- (42) Ben-Avraham, D. *Phys. Rev. B* **1993**, *47*, 14559–14560.
- (43) Levitt, M.; Sander, C.; Stern, P. S. *J. Mol. Biol.* **1985**, *181*, 423–447.
- (44) Edwards, C.; Palmer, S. B.; Emsley, P.; Helliwell, J. R.; Glover, I. D.; Harris, G. W.; Moss, D. S. *Acta Crystallogr., Sect. A: Found. Crystallogr.* **1990**, *46*, 315–320.
- (45) Sette, F.; Ruocco, G.; Krisch, M.; Masciovecchio, C.; Verbeni, R.; Bergmann, U. *Phys. Rev. Lett.* **1996**, *77*, 83–86.
- (46) Santucci, S. C.; Fioretto, D.; Comez, L.; Gessini, A.; Masciovecchio, C. *Phys. Rev. Lett.* **2006**, *97*, 225701.
- (47) Walrafen, G. E.; Chu, Y. C.; Piermarini, G. J. *J. Phys. Chem.* **1996**, *100*, 10363–10372.
- (48) Schober, H.; Koza, M. M.; Masciovecchio, C.; Sette, F.; Fujara, F. *Phys. Rev. Lett.* **2000**, *85*, 4100–4103.
- (49) Cornicchi, E.; Sebastiani, F.; De Francesco, A.; Orecchini, A.; Paciaroni, A.; Petrillo, C.; Sacchetti, F. *J. Chem. Phys.* **2011**, *135*, 025101.
- (50) Green, J. L.; Fan, J.; Angell, C. A. *J. Phys. Chem.* **1994**, *98*, 13780–13790.
- (51) Shakhnovich, E. I.; Finkelstein, A. V. *Biopolymers* **1989**, *28*, 1667–1680.
- (52) Tsai, J.; Taylor, R.; Chothia, C.; Gerstein, M. *J. Mol. Biol.* **1999**, *290*, 253–266.
- (53) Gerstein, M.; Chothia, C. *Proc. Natl. Acad. Sci. U.S.A.* **1996**, *93*, 10167–10172.
- (54) Zhou, Y.; Vitkup, D.; Karplus, M. *J. Mol. Biol.* **1999**, *285*, 1371–1375.